



OPEN

Scalable and selective deuteration of (hetero)arenes

Wu Li¹, Jabor Rabeah¹, Florian Bourriquen¹, Dali Yang², Carsten Kreyenschulte¹, Nils Rockstroh¹, Henrik Lund¹, Stephan Bartling¹, Annette-Enrica Surkus¹, Kathrin Junge¹, Angelika Brückner¹✉, Aiwen Lei²✉ and Matthias Beller¹✉

Isotope labelling, particularly deuteration, is an important tool for the development of new drugs, specifically for identification and quantification of metabolites. For this purpose, many efficient methodologies have been developed that allow for the small-scale synthesis of selectively deuterated compounds. Due to the development of deuterated compounds as active drug ingredients, there is a growing interest in scalable methods for deuteration. The development of methodologies for large-scale deuterium labelling in industrial settings requires technologies that are reliable, robust and scalable. Here we show that a nanostructured iron catalyst, prepared by combining cellulose with abundant iron salts, permits the selective deuteration of (hetero)arenes including anilines, phenols, indoles and other heterocycles, using inexpensive D₂O under hydrogen pressure. This methodology represents an easily scalable deuteration (demonstrated by the synthesis of deuterium-containing products on the kilogram scale) and the air- and water-stable catalyst enables efficient labelling in a straightforward manner with high quality control.

Isotope labelling methodologies play an essential part in the development of new pharmaceuticals and agrochemicals¹ (Fig. 1a). For example, in the pharmaceutical industry, isotopes of active drugs are commonly prepared to understand their metabolism and to identify specific metabolites (Fig. 1b). The most common isotopic labels are deuterium atoms, which are also well suited to determine kinetic isotope effects (KIEs) in fundamental mechanistic investigations that result from differences in the rate of C–H versus C–D bond cleavage^{2,3} (Fig. 1c). Deuterium-labelled compounds show virtually identical physical behaviour to that of their hydrogen analogues, whilst differing in molecular mass, and thus are the primary source for the preparation of internal standards for liquid chromatography–mass spectrometry (LC–MS) analysis in the investigation of environmental, animal and human samples^{4,5} (Fig. 1d). Accordingly, deuteration facilitates advancements in metabolomics including metabolite identification and quantification, in toxicogenomic studies for the related reactive metabolites and in proteomics studies.

Due to the potentially improved pharmacokinetic and pharmacological properties of deuterium-labelled compounds, while retaining almost the same chemical structure and physical properties as the unlabelled counterparts, in recent years this class of compounds has gained increasing interest as actual medications^{6,7}. Notably, in 2017 the Food and Drug Administration (FDA) cleared the first deuterated drug, Austedo, for the treatment of Huntington's-disease-related disorders⁸. Meanwhile, several deuterated compounds are in clinical trials for various applications. Based on these developments, there is growing potential and interest in accessing selectively deuterated building blocks on a larger scale. In this context, specific and practical labelling methodologies for arenes/heteroarenes as well as amines, which are found in most small-molecule-based drugs, are of increasing importance. Critical parameters for such applications are the availability and price of the

labelling reagent, catalysts and so on, and the feasibility of the process in an industrial setting. Notably, precise control of impurities, degree of deuteration and consistency are also prerequisites for any real-life implementation⁹.

Acid-mediated hydrogen–deuterium exchange reactions (H/D exchange) are among the oldest methods known for labelling of arenes. Nevertheless, they allow selective incorporation of deuterium only for simple substrates following an electrophilic aromatic substitution mechanism (Fig. 1e)¹⁰. In most of the known protocols, the necessity to use high temperatures and stoichiometric amounts of concentrated strong acids leads to poor functional group tolerances and safety risks, especially on a larger scale¹¹.

Based on advances in homogeneous metal-catalysed C–H activation, a variety of organometallic complexes have evolved for catalytic H/D exchange reactions of arenes, as well as aliphatic amines in the α or β positions (Fig. 1f)^{12–15}. For example, homogeneous iridium-based Crabtree and Kerr catalysts have been used for C(sp²)–H hydrogen isotope exchange reactions using D₂ gas^{16,17}. Chirik and co-workers first reported the use of a molecularly defined iron catalyst for the tritiation/deuteration of pharmaceutical drugs at aromatic C–H moieties using D₂ and T₂ gas¹⁸. More recently, the MacMillan group developed a photochemical-catalysed hydrogen-isotope-exchange (HIE) method for the selective labelling of *N*-alkylamine-based drugs¹⁹.

Apart from photocatalysts and defined organometallic complexes, heterogeneous materials have also been studied in labelling reactions. So far, Pd/C and Pt/C are known to catalyse multi H/D exchange of arenes and heterocyclic amines²⁰. In addition, ruthenium- and iridium-based catalysts in the presence of D₂ have been developed with promising activity^{21,22}. Unfortunately, in all these cases the selectivity and the tolerance of easily reducible functional groups and halogens is challenging. Furthermore, besides those based on nickel²³, all heterogeneous catalysts known

¹Leibniz-Institut für Katalyse e.V., Rostock, Germany. ²Institute for Advanced Studies (IAS), Wuhan University, Wuhan, P. R. China.

✉e-mail: angelika.brueckner@catalysis.de; aiwenlei@whu.edu.cn; matthias.beller@catalysis.de

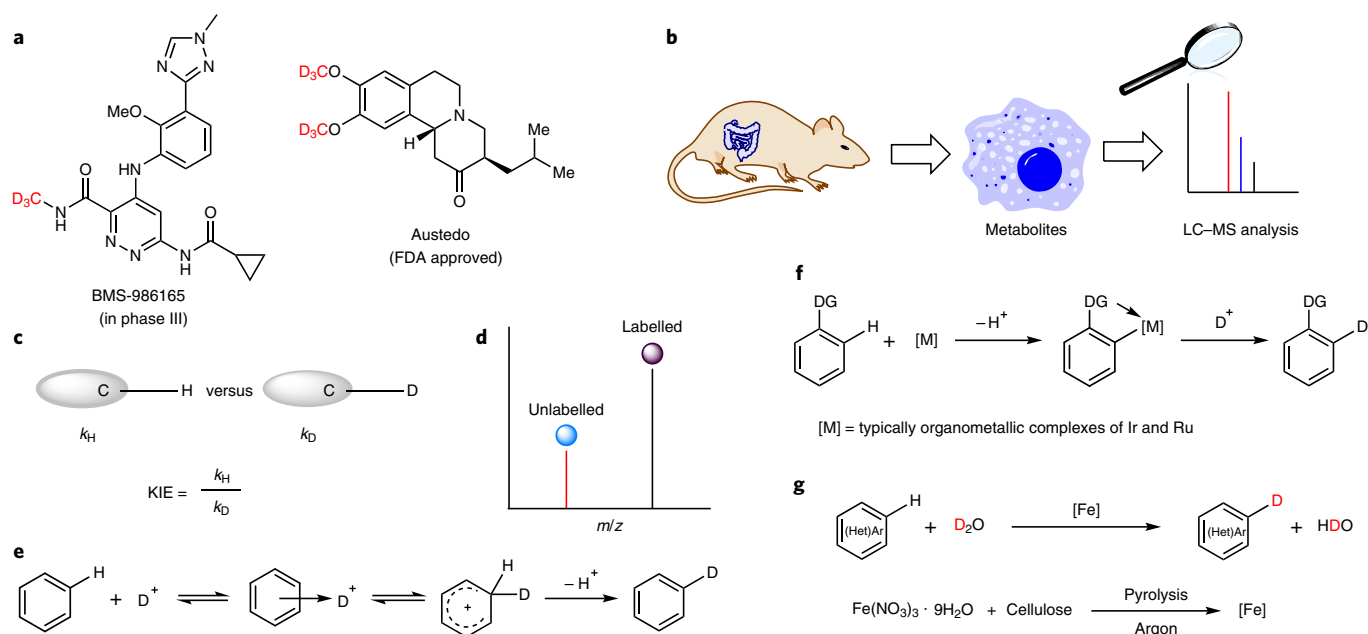


Fig. 1 | Applications of deuteration and methods for H/D exchange. **a**, Deuterated drug molecules: Austedo has been approved by the FDA and BMS-986165 is under trial. **b**, Identification of specific metabolites using LC-MS: accurate analysis of metabolites based on stable isotope labelling coupled with LC-MS analysis. **c**, KIE investigations based on C-H versus C-D bond cleavage. **d**, Preparation of internal standards for LC-MS analysis. The isotopically labelled internal standards can be used for quantitative determination. **e**, Acid-mediated H/D exchange. **f**, Transition-metal-catalysed H/D exchange. DG, directing group. **g**, This work: nanostructured iron catalyst for H/D exchange of (hetero)arenes using D_2O .

for deuteration rely on expensive precious metals, which hamper their use in the agrochemical, pharmaceutical or food industries as those metals must be removed completely from the final products according to regulations. Apart from the catalyst and the reaction conditions, the source of deuterium is critical for the application of such methodologies. This is especially true for the preparation of labelled building blocks on the multi-gram or even kilogram scale. In this respect, cheap, safe and operationally convenient D_2O is the ideal source for such transformations because it is basically the parent compound for all other deuteration reagents, including D_2 .

In this article we report a unique heterogeneous iron catalyst for general and practical deuteration of arenes and heteroarenes. Using D_2O in the presence of a biomass-derived iron catalyst under hydrogen pressure allows for the preparation of >90 selectively deuterated building blocks, representative drugs and natural products with high and reliable deuterium incorporation (Fig. 1g).

Results and discussion

Reaction development. Initially, we tested standard, commercially available heterogeneous catalysts and tailor-made supported nanoparticles (NPs) for selective deuteration of 4-phenylmorpholine in D_2O (Supplementary Table 1). This benchmark substrate was chosen because it permits labelling both at the nitrogen-containing heterocycle and the phenyl ring. In all cases, the extent of isotopic exchange was determined using 1H NMR spectroscopy. In agreement with previous works²⁴, Pd/C led to deuterium incorporation at the α position of the nitrogen atom on the morpholine ring (Supplementary Table 1, entry 1). Recently, we introduced a variety of supported 3d-metal NPs for selective hydrogenation and oxidation reactions^{25,26}. In this context, iron-based NPs are particularly attractive to us due to the abundance, low cost and negligible safety concerns of iron salts. Much to our surprise, pyrolysis of $Fe(NO_3)_3 \cdot 9H_2O$ with cellulose resulted in highly active and selective catalytic systems for deuteration of the phenyl ring in the *ortho* and *para* positions, which even outperformed commercial

catalysts such as Pt/C, Au/C and Ru/C (Supplementary Table 1, entry 10 versus entries 2 and 4). The deuterium incorporation could be further improved under hydrogen pressure (Supplementary Table 1, entry 12). Furthermore, the stability and recyclability of the catalyst under H_2 are better (Supplementary Information, section 5). Pseudo in situ X-ray photoelectron spectroscopy (XPS) studies show that the iron oxides formed on the surface of the catalyst during the catalysis could be partially reduced to Fe(0) when heating the sample under H_2 (Supplementary Fig. 6). Finally, the benchmark reaction performed with D_2O in the presence of hydrogen at 120 °C gave nearly quantitative deuteration (see Supplementary Table 1 for more details).

Catalyst characterization. To understand the structure of the most active material (Fe-Cellulose-1000), powder X-ray diffraction, XPS, scanning transmission electron microscopy (STEM) and X-ray absorption spectroscopy (XAS) investigations were performed. These results show that the freshly pyrolysed catalyst consists of Fe/ Fe_3C particles 20–50 nm in size, covered by a shell of up to 30 graphene layers with an overall thickness of 6–10 nm. Embedding the particles in the carbon matrix prevents them from undesired aggregation. During the early stages of the catalytic reaction, the graphene cover is partly removed, thus enabling the contact of the iron surface with reactants. Then, during the reaction, Fe_3C is partly converted to metallic iron which is considered as active phase in the reaction (for details see Supplementary Information, section 6).

Mechanistic studies. Next, investigations of KIE and electron paramagnetic resonance (EPR) studies were performed to obtain a better mechanistic understanding (Supplementary Information, section 7). According to comparison experiments of the model substrate, the reaction is roughly four times faster in H_2O than in D_2O . Apparently, the cleavage of the D-OD bond is the rate-limiting step in this process (Fig. 2a and Supplementary Fig. 13). Interestingly, by comparing the deuteration of aniline and 3,5-dideuterioaniline, a

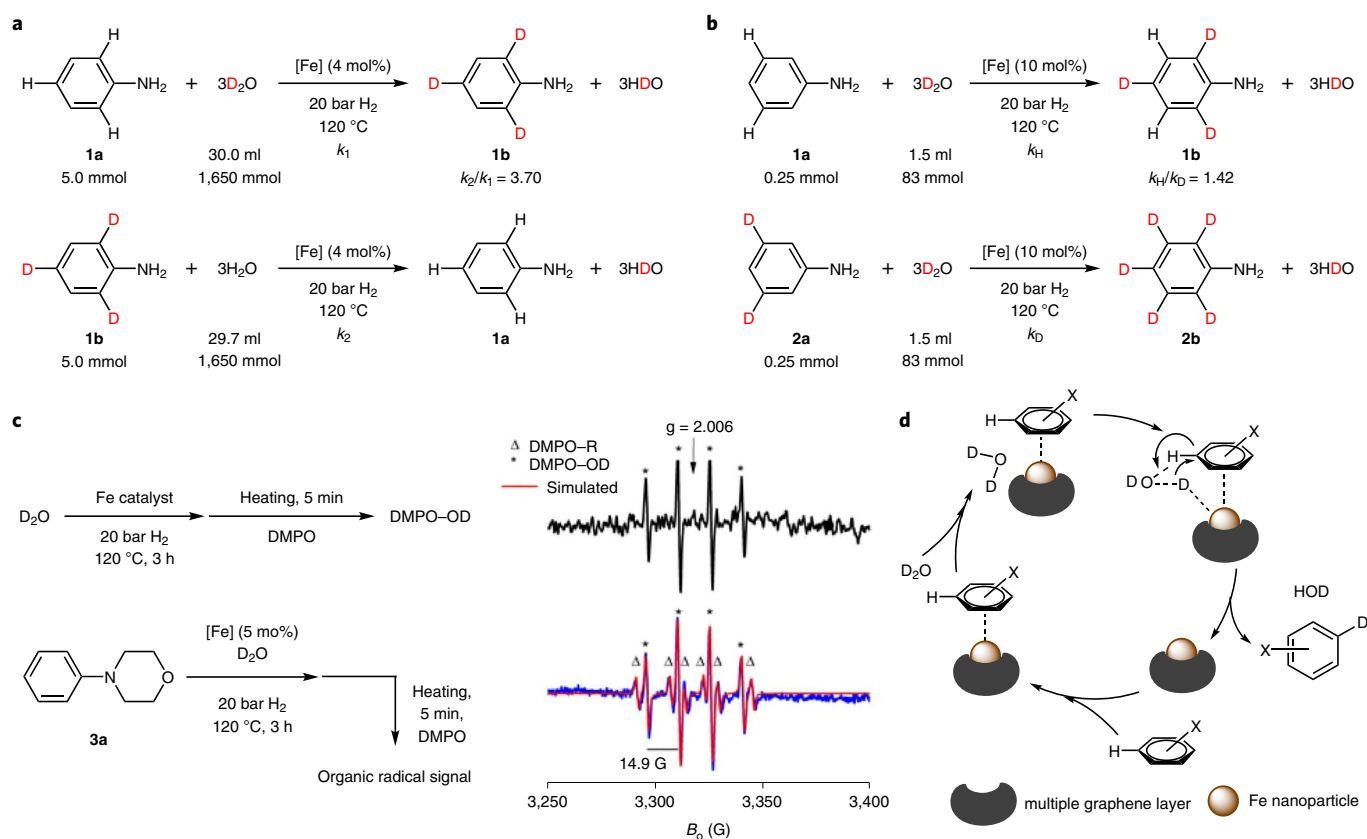


Fig. 2 | Mechanistic studies and proposed mechanism. **a**, Aniline in D_2O and aniline-2,4,6- d_3 in H_2O were used for the KIE studies. The reaction in H_2O is roughly four times faster than the reaction in D_2O . **b**, Deuteration of aniline and 3,5-dideuterioaniline in D_2O were performed for KIE studies, and a minor secondary KIE was observed. **c**, EPR studies: $\cdot\text{OD}$ radical trapping using DMPO and detection of the DMPO-R spin adduct. This indicates that formation of radical intermediates is a consequence of homolytic D-OD scission initiated by the iron catalyst. **d**, Proposed mechanism: the multiple graphene layer is removed during the early stages of the catalytic reaction, thus enabling contact of the iron surface with D_2O and reactants. The key step of the reaction is D_2O splitting by the iron catalyst. The resulting radicals are not liberated into the solution but remain adsorbed on the catalyst surface.

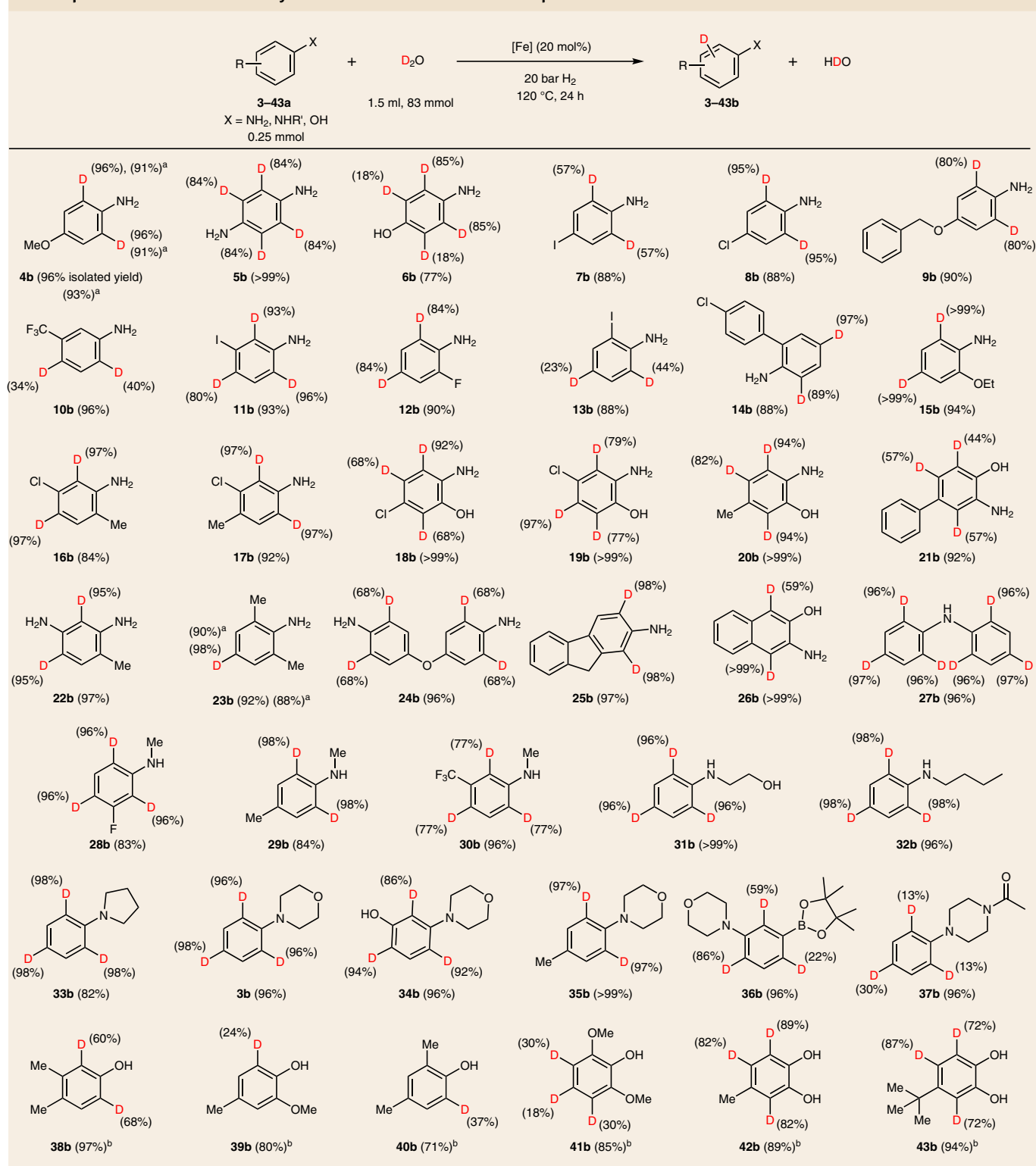
minor secondary KIE is also observed (Fig. 2b and Supplementary Fig. 14). This kinetically relevant result may be explained by the slightly different coordination of the deuterated and non-deuterated substrate to active catalyst centres on the surface. To check whether radicals are formed upon cleavage of the D-OD bond, EPR measurements with the spin trap 5,5-dimethyl-1-pyrroline-*N*-oxide (DMPO) have been performed (Supplementary Information, section 7.2). In a blind experiment, the catalyst was heated in D_2O before DMPO was added, and an EPR spectrum was recorded immediately after quenching the reaction to room temperature. This spectrum showed only a weak but characteristic hyperfine structure quartet signal of DMPO-OD spin adducts²⁷ which results from trapping $\cdot\text{OD}$ radicals by DMPO (Fig. 2c black line). This shows that the iron catalyst can promote to a small extent homolytic splitting of D_2O . However, in the presence of 4-phenylmorpholine, an additional hyperfine structure sextet characteristic of a DMPO-R spin adduct²⁸ was detected (Fig. 2c, blue line), suggesting that $\cdot\text{OD}$ subtract hydrogen atoms from the substrate, forming HOD, leaving behind $\cdot\text{R}$ radicals. Interestingly, no $\cdot\text{R}$ radicals were detected when the iron catalyst and the 4-phenylmorpholine substrate were heated in toluene, which indicates that formation of radical intermediates is a consequence of homolytic D-OD scission initiated by the iron catalyst. Considering the well-known fact that $\cdot\text{OD}$ radicals are very reactive and unselective, the observed high selectivity is surprising.

Proposed mechanism. We propose a concerted mechanism in which D_2O is split homogeneously by the iron catalyst, yet the

resulting radicals are not liberated into the solution but remain adsorbed on the catalyst surface as activated D^* and $\cdot\text{OD}$ species. $\cdot\text{OD}$ abstracts a hydrogen atom from the phenyl ring, forming HDO and the corresponding phenyl \cdot species^{29,30}, which subsequently produces D-R (Fig. 2c,d). The observed high *ortho/para* selectivity may be a result of electron density transfer from the electron-rich metallic iron particle to the adsorbed aromatic ring because this is well known to promote electrophilic *ortho/para* substitutions.

Synthetic scope. Building blocks. Having established the optimized conditions, we then evaluated the substrate scope of the system and its tolerance towards functional groups. Because anilines are used for the synthesis of diverse building blocks for agrochemicals and pharmaceuticals, we started to explore the deuteration of functionalized anilines. Indeed, Fe-Cellulose-1000 permitted smooth deuteration of 35 different anilines with excellent chemo- and regioselectivity (Table 1, 3–37b).

In general, the transformations can be easily run on the gram-scale (4b and 23b). Diverse halogen-containing (for example, chlorine and iodine) anilines afforded the deuterated products (7b, 8b, 11–14b and 16–19b) without notable dehalogenation side-reactions, which is a common problem of precious-metal-based catalysts. We demonstrated the isotopic purity of chloro-, bromo- and iodo-containing compounds by LC-MS (Supplementary Information, section 8.3). Furthermore, deuteration of some phenols in the presence of the iron catalyst showed deuterium incorporation after an extended time (Table 1,

Table 1 | Nanostructured iron catalyst for deuteration of anilines and phenols

Deuterium content determined by quantitative ¹H NMR. ^aThe reaction was performed on the gram scale. ^bThe reaction time was 72 h.

38–43b). Like the model system, negligible or no deuterium incorporation is observed for several representative substrates (**3a**, **4a**, **38a**, **44a**, **52a** and **67a**) in the absence of the iron catalyst (Supplementary Fig. 16).

Next, deuteration of different nitrogen-containing heteroarenes such as pyridines, tetrahydroquinolines, phenothiazines, phenoxazines, indoles, indolines and quinolines, and even those

bearing two nitrogen atoms, were investigated. Such heterocycles are representative structural components of modern pharmaceuticals: 59% of FDA-approved drugs contain a nitrogen heterocyclic motif³¹. As shown in Table 2, catalytic labelling provided the corresponding products (**44–66b**). Notably, for anilines and phenols the regioselectivity of the labelling reaction is in accordance with an electrophilic aromatic substitution mechanism. However,

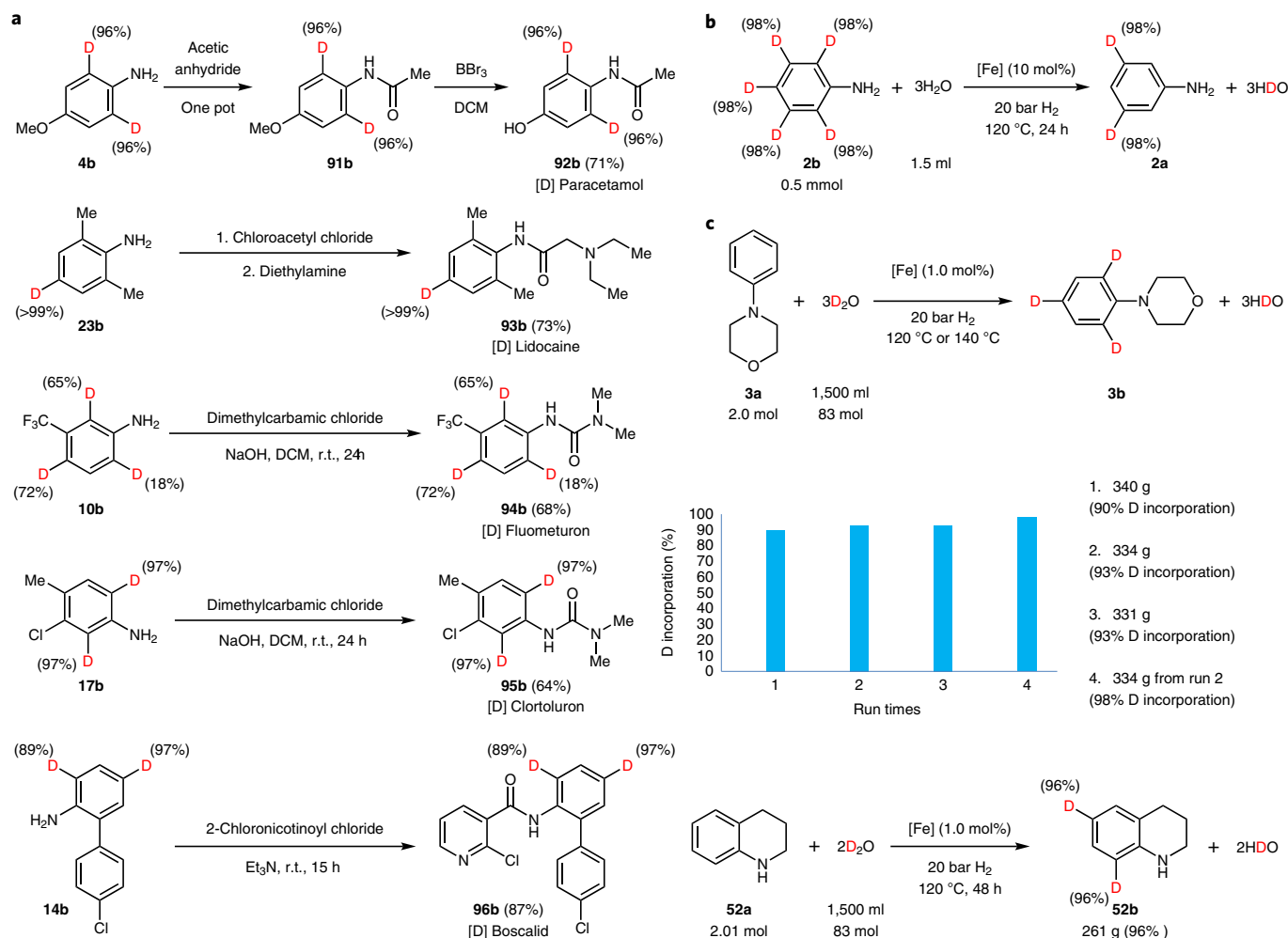


Fig. 3 | Synthetic applications and large-scale synthesis. **a**, Preparation of deuterated *N*-acylated anilines. Deuterated drugs, herbicides and fungicide were prepared from the corresponding deuterated anilines. **b**, Dedeuteration of perdeuterated aniline using H₂O to 3,5-dideuterioaniline. **c**, Scale-up reactions: reuse of the iron catalyst on the 2.0 mol scale. Overall, 1.005 kg 4-phenylmorpholine (6.17 mol) was deuterated using the same catalyst batch; >95% deuterium-labelled 4-phenylmorpholine and 1,2,3,4-tetrahydroquinoline were produced.

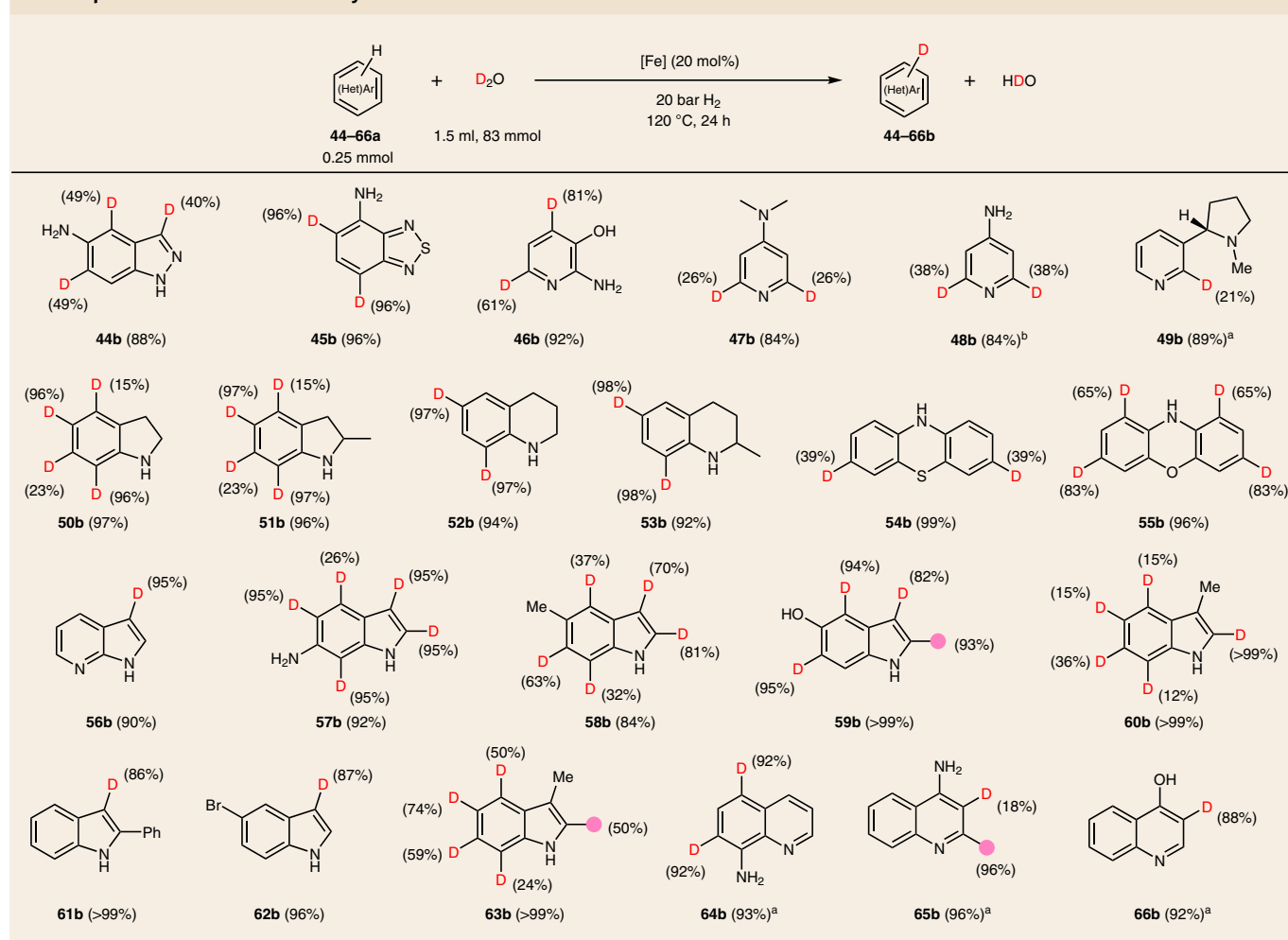
using pyridines, indoles or indolines, different reactivity patterns are observed, which hints towards a different process.

Natural products and pharmaceuticals. To further showcase the utility of iron-catalysed H/D exchange reactions, late-stage deuteration of representative drugs and natural products was investigated (Table 3). For example, melatonin is converted into the deuterated **67b** with high levels of deuterium incorporation. Similarly, *N*-acetylserotonin is deuterated to give **68b**. Purine-containing compounds, such as nucleoside analogues kinetin, inosine, pentoxifylline and the nucleobase adenine, are labelled to the products **69–71b** and **73b**. Alkaloids, for example, brucine and strychnine, are deuterated at both aromatic rings and in the heterocyclic ring in the α position to the nitrogen (**74b** and **75b**). In the case of nicotinic acid, labelling occurred with relatively lower deuterium incorporation selectively to give **76b**. Furthermore, natural phenol derivatives, for example, tyrosol, resveratrol, thymol, arbutin and piceid, were evaluated (**77–81b**). Tetrahydroquinoline alkaloids, for example, augustureine and galipinine, also proceeded with deuterium labelling (**82b** and **83b**). Aniline derivatives such as dropropizine, DL-aminogluthethimide and nimodipine-NH₂ were deuterated with good selectivity (**84–86b**). Notably, medications such as carvedol, estradiol and

O-desmethylvenlafaxine gave the deuterium analogues **87–89b**. As an example, for selective deuteration of an aromatic amino acid, L-tryptophan was employed to directly give **90b**. In all cases shown above the standard catalytic protocol was used and no further optimization was performed. However, it should be noted that the deuterium incorporation can be substantially improved at higher temperature (**84b** and **90b**).

Following standard conditions, deuteration of *N*-acylated anilines is more difficult; however, such labelled products can be conveniently prepared from the corresponding deuterated anilines (Fig. 3a). For instance, 2,6-D-labelled paracetamol **92b** was readily synthesized with excellent deuterium incorporation. Deuterated lidocaine **93b**, herbicides fluometuron **94b** and chlortoluron **95b** as well as fungicide boscalid **96b** were obtained from the corresponding deuterated anilines.

All these cases demonstrate that the presented methodology works well with amino- and/or hydroxyl-substituted arenes as well as heteroarenes; however, less electron-rich benzenes, for example, 1-bromo-, 1-chloro- and 1-fluoro-4-methoxybenzene and 1-methyl-4-(trifluoromethyl)benzene, showed no notable deuterium incorporation under standard conditions. In case of successful labelling as described above deuteration occurred at the most

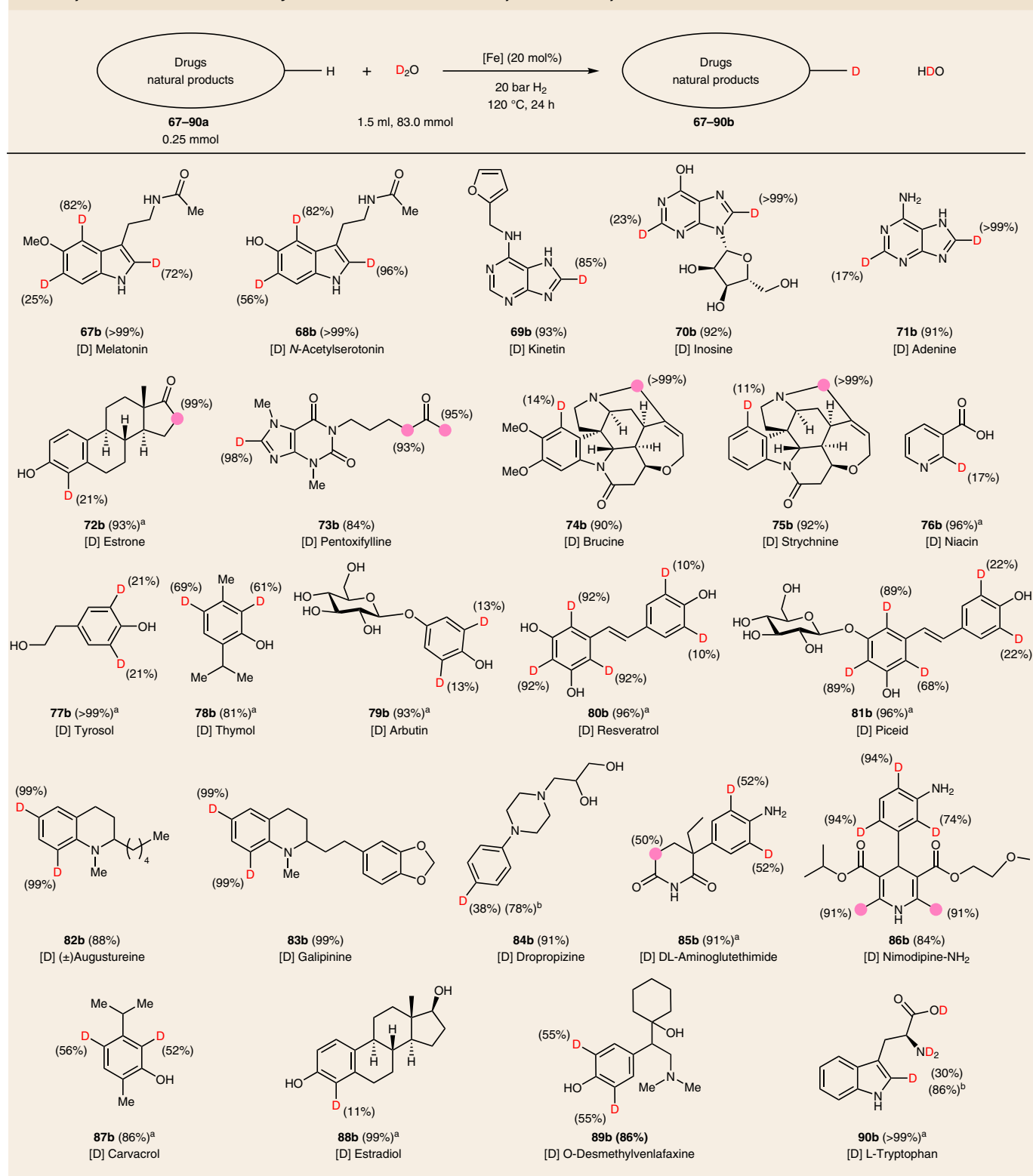
Table 2 | Nanostructured iron catalyst for deuteration of heteroarenes

electron-rich positions. Obviously, this limits the possibilities to obtain deuterated compounds at other positions. For example, 2,4,6-trideuterated anilines are conveniently available, while selective deuteration at the 3- and 5-positions are apparently not possible. However, we envisioned a convenient strategy to overcome this limitation: non-selective deuteration of anilines is known in the presence of Pt/C (ref. ³²). Subsequent selective D/H exchange using our Fe-Cellulose-1000 catalyst in water makes it possible to selectively obtain deuterium isomers at positions that are not prone to electrophilic substitution reactions. Thus, 3,5-dideuterioaniline **2a** is obtained from aniline via the perdeuterated derivative (Fig. 3b).

Having established complementary approaches for selective deuteration of a variety of substrates, we then evaluated some practical aspects of our catalyst system. It should be noted that most of the reactions shown above have been performed on a scale typically used in drug discovery. However, as shown in Fig. 3c it is possible to conveniently run such labelling reactions on the 20 to >300 g scale (Supplementary Information, section 9), with the only limitation being the size of the commercial autoclave. In general, stability, reusability and avoidance of metal contamination are intrinsic advantages to the use of any heterogeneous catalyst. To demonstrate these benefits, the iron catalyst was recycled up to five times for the benchmark reaction. As depicted in Supplementary Fig. 18, no substantial loss of activity was observed. During deuteration reactions, an oxidic structure composed of Fe²⁺ and Fe³⁺ was formed as proven by XPS (Supplementary Fig. 5). With respect to metal contamination of the

product, inductively coupled plasma optical emission spectrometry measurements of the D₂O solution detected no iron leaching in any of these runs (Supplementary Table 8). Notably, the recycled catalyst system can also be used for different substrates, which is important in the context of multipurpose batch reactors, which dominate in the pharmaceutical industry. Thus, labelled products with high deuterium incorporation were produced on >1 kg scale from the same catalyst batch (Fig. 3c and Supplementary Information, section 9).

In summary, we have developed a general methodology for heterogeneous iron-catalysed deuteration reactions. We believe this protocol paves the way for practical labelling processes and the large-scale synthesis of specific deuterated building blocks. Although the quality of different deuteration reactions was performed as accurately as possible (Supplementary Tables 5 and 6), all presented developments took place under conditions that did not conform to good manufacturing practice. The optimal biomass-derived catalyst allows for an activation and utilization of low-cost D₂O. The performance of this catalyst system is improved in the presence of hydrogen, which leads to in situ reduction of iron oxides on the surface as indicated by pseudo in situ XPS measurements (Supplementary Fig. 6). The presented system is effective for the selective deuteration of anilines, indoles, phenols and other heterocyclic compounds, including late-stage labelling of natural products and bioactive molecules, and can be readily used for the preparation of deuterated compounds on the kilogram scale. By using complementary approaches, different positional deuterated products can also be obtained in a practical manner.

Table 3 | Nanostructured iron catalyst for deuteration of natural products and pharmaceuticals

Representative drugs, hormones, nucleobases, steroids, alkaloids, amino acids, upscale and applications. Deuterium content determined by quantitative ¹H NMR. ^aThe reaction time was 72 h. ^bThe reaction was performed at 140 °C for 24 h. The pink circles and numbers denote the positions of the C-H bonds that are labelled and the percentage incorporation of the hydrogen isotope, respectively.

Online content

Any methods, additional references, Nature Research reporting summaries, source data, extended data, supplementary information, acknowledgements, peer review information; details of author contributions and competing interests; and statements of

data and code availability are available at <https://doi.org/10.1038/s41557-021-00846-4>.

Received: 27 October 2020; Accepted: 25 October 2021;
Published online: 13 January 2022

References

1. Prechtl, M. H., Teltewskoi, M., Dimitrov, A., Kemnitz, E. & Braun, T. Catalytic C–H bond activation at nanoscale Lewis acidic aluminium fluorides: H/D exchange reactions at aromatic and aliphatic hydrocarbons. *Chem. Eur. J.* **17**, 14385–14388 (2011).
2. Simmons, E. M. & Hartwig, J. F. On the interpretation of deuterium kinetic isotope effects in C–H bond functionalizations by transition-metal complexes. *Angew. Chem. Int. Ed.* **51**, 3066–3072 (2012).
3. Zhan, M. et al. A simple and cost-effective method for the regioselective deuteration of phenols. *Eur. J. Org. Chem.* **2015**, 3370–3373 (2015).
4. Smith, J. A. et al. Preparation of cyclohexene isotopologues and stereoisotopomers from benzene. *Nature* **581**, 288–293 (2020).
5. Atzrodt, J., Deraud, V., Fey, T. & Zimmermann, J. The renaissance of H/D exchange. *Angew. Chem. Int. Ed.* **46**, 7744–7765 (2007).
6. Sanderson, K. Big interest in heavy drugs. *Nature* **458**, 269 (2009).
7. Katsnelson, A. Heavy drugs draw heavy interest from pharma backers. *Nat. Med.* **19**, 656 (2013).
8. Schmidt, C. First deuterated drug approved. *Nat. Biotechnol.* **35**, 493–494 (2017).
9. Czeskis, B. et al. Deuterated active pharmaceutical ingredients: a science-based proposal for synthesis, analysis, and control. Part 1: Framing the problem. *J. Labelled Comp. Radiopharm.* **62**, 690–694 (2019).
10. Martins, A. & Lautens, M. A simple, cost-effective method for the regioselective deuteration of anilines. *Org. Lett.* **10**, 4351–4353 (2008).
11. Magano, J. & Dunetz, J. R. Large-scale applications of transition metal-catalyzed couplings for the synthesis of pharmaceuticals. *Chem. Rev.* **111**, 2177–2250 (2011).
12. Atzrodt, J., Deraud, V., Kerr, W. J. & Reid, M. C–H functionalisation for hydrogen isotope exchange. *Angew. Chem. Int. Ed.* **57**, 3022–3047 (2018).
13. Hesk, D. Highlights of C(sp²)–H hydrogen isotope exchange reactions. *J. Labelled Comp. Radiopharm.* **63**, 247–265 (2020).
14. Qiao-Xia, G., Bao-Jian, S., Hai-Qing, G. & Tamotsu, T. Aromatic H/D exchange reaction catalyzed by groups 5 and 6 metal chlorides. *Chin. J. Chem.* **23**, 341–344 (2005).
15. Müller, V., Weck, R., Deraud, V. & Ackermann, L. Ruthenium(II)-catalyzed hydrogen isotope exchange of pharmaceutical drugs by C–H deuteration and C–H tritiation. *ChemCatChem* **12**, 100–104 (2019).
16. Crabtree, R. H., Felkin, H. & Morris, G. E. Cationic iridium diolefin complexes as alkene hydrogenation catalysts and the isolation of some related hydrido complexes. *J. Organomet. Chem.* **141**, 205–215 (1977).
17. Nilsson, G. N. & Kerr, W. J. The development and use of novel iridium complexes as catalysts for *ortho*-directed hydrogen isotope exchange reactions. *J. Labelled Comp. Radiopharm.* **53**, 662–667 (2010).
18. Yu, R. P., Hesk, D., Rivera, N., Pelczar, I. & Chirik, P. J. Iron-catalysed tritiation of pharmaceuticals. *Nature* **529**, 195–199 (2016).
19. Loh, Y. Y. et al. Photoredox-catalyzed deuteration and tritiation of pharmaceutical compounds. *Science* **358**, 1182–1187 (2017).
20. Sajiki, H., Sawama, Y. & Monguchi, Y. Efficient H–D exchange reactions using heterogeneous platinum-group metal on carbon–H₂–D₂O System. *Synlett* **23**, 959–972 (2012).
21. Pieters, G. et al. Regioselective and stereospecific deuteration of bioactive aza compounds by the use of ruthenium nanoparticles. *Angew. Chem. Int. Ed.* **53**, 230–234 (2014).
22. Valero, M. et al. NHC-stabilized iridium nanoparticles as catalysts in hydrogen isotope exchange reactions of anilines. *Angew. Chem. Int. Ed.* **59**, 3517–3522 (2020).
23. Heys, J. R. Nickel-catalyzed hydrogen isotope exchange. *J. Labelled Comp. Radiopharm.* **53**, 716–721 (2010).
24. Sajiki, H. et al. Efficient and selective deuteration of phenylalanine derivatives catalyzed by Pd/C. *Synlett* **2005**, 0845–0847 (2005).
25. Jagadeesh, R. V. et al. Nanoscale Fe₂O₃-based catalysts for selective hydrogenation of nitroarenes to anilines. *Science* **342**, 1073–1076 (2013).
26. Cui, X. et al. Synthesis and characterization of iron-nitrogen-doped graphene/core-shell catalysts: efficient oxidative dehydrogenation of N-heterocycles. *J. Am. Chem. Soc.* **137**, 10652–10658 (2015).
27. Belhadj, H., Melchers, S., Robertson, P. K. J. & Bahnemann, D. W. Pathways of the photocatalytic reaction of acetate in H₂O and D₂O: a combined EPR and ATR-FTIR study. *J. Catal.* **344**, 831–840 (2016).
28. Dai, X. et al. Sustainable co-synthesis of glycolic acid, formamides and formates from 1,3-dihydroxyacetone by a Cu/Al₂O₃ catalyst with a single active sites. *Angew. Chem. Int. Ed.* **58**, 5251–5255 (2019).
29. Mader, E. A., Davidson, E. R. & Mayer, J. M. Large ground-state entropy changes for hydrogen atom transfer reactions of iron complexes. *J. Am. Chem. Soc.* **129**, 5153–5166 (2007).
30. Barckholtz, C., Barckholtz, T. A. & Hadad, C. M. A mechanistic study of the reactions of H, O (3P), and OH with monocyclic aromatic hydrocarbons by density functional theory. *J. Phys. Chem. A* **105**, 140–152 (2001).
31. Vitaku, E., Smith, D. T. & Njardarson, J. T. Analysis of the structural diversity, substitution patterns, and frequency of nitrogen heterocycles among US FDA approved pharmaceuticals. *J. Med. Chem.* **57**, 10257–10274 (2014).
32. Ito, N. et al. Efficient and selective Pt/C-catalyzed H–D exchange reaction of aromatic rings. *Bull. Chem. Soc. Jpn.* **81**, 278–286 (2008).

Publisher's note Springer Nature remains neutral with regard to jurisdictional claims in published maps and institutional affiliations.



Open Access This article is licensed under a Creative Commons Attribution 4.0 International License, which permits use, sharing, adaptation, distribution and reproduction in any medium or format, as long as you give appropriate credit to the original author(s) and the source, provide a link to the Creative Commons license, and indicate if changes were made. The images or other third party material in this article are included in the article's Creative Commons license, unless indicated otherwise in a credit line to the material. If material is not included in the article's Creative Commons license and your intended use is not permitted by statutory regulation or exceeds the permitted use, you will need to obtain permission directly from the copyright holder. To view a copy of this license, visit <http://creativecommons.org/licenses/by/4.0/>.

© The Author(s) 2022

Methods

Determination of deuterium incorporation. The positions and percentage of deuterium incorporation were determined by ^1H NMR. The equation below was used to determine the degree of deuterium incorporation; peaks were calibrated against a signal corresponding to an unlabelled position. The labelling position was determined by ^1H NMR according to the chemical shifts and peak multiplicity. In addition, deuterium incorporations were confirmed using high-resolution MS by comparison of all the labelled and unlabelled compounds (note that high-resolution MS serves here to substantiate the results of quantitative NMR analysis).

$$\% \text{ deuteration} = 100 - \left[\left(\frac{\text{residual integral}}{\text{number of labelling sites}} \times 100 \right) \right]$$

Procedure for the preparation of the catalyst. A 250 ml oven-dried single-necked round-bottomed flask equipped with a reflux condenser and a Teflon-coated, egg-shaped magnetic stir bar (40 mm \times 18 mm) was charged with $\text{Fe}(\text{NO}_3)_3 \cdot 9\text{H}_2\text{O}$ (404 mg, 1.0 mmol) dissolved in ethanol (150 ml). Then, this solution was heated to 80 °C (r.t. to 80 °C) in an oil bath and stirred for 1 h. To the reaction solution, 6.0 g cellulose was added via a glass funnel, and the resulting heterogeneous mixture was stirred at 450 r.p.m. for 15 h at 80 °C. The flask was taken out from the bath and cooled to ambient temperature. The solvent was removed in vacuum and then dried under an oil pump vacuum for 4 h to give a yellow solid. The sample was transferred to a ceramic crucible and placed in an oven. The latter was evacuated to ~ 5 mbar and then flushed with argon three times. The furnace was heated to 1,000 °C at a rate of 25 °C min^{-1} and held at 1,000 °C for 2 h under argon atmosphere. After the heating was switched off, the oven was allowed to reach r.t., giving the Fe-Cellulose-1000 catalyst as a black powder (note that throughout the process, argon was constantly passed through the oven).

General procedure for the deuteration reactions. In a 4 ml vial fitted with a magnetic stir bar and septum cap, iron catalyst (60 mg, 20 mol%) and substrate (0.25 mmol) were added. Then, a needle was inserted in the septum, allowing gaseous reagents to enter. After adding the solvent deuterium oxide (1.5 ml), the vials (up to eight) were set in an alloy plate and then placed into a 300 ml steel Parr autoclave. The autoclave was flushed with hydrogen six times at 10 bar and finally pressurized to the desired value (20 bar). Then, it was placed into an aluminium block and heated to the desired temperature. At the end of the reaction, the autoclave was quickly cooled down to r.t. with an ice bath and vented. Finally, the samples were removed from the autoclave, and ethyl acetate was added to the crude mixture. This mixture was centrifuged, and the organic layer was removed from the vials (three times). After removal of all volatiles in vacuo, the desired products were obtained. In case of anilines with deuterium labelling on the nitrogen, 1 ml H_2O was added during work up and N–D was replaced by N–H.

General procedure for the >300 g scale reactions. To a 2 l steel Parr autoclave containing 28.0 g Fe-Cellulose-1000 catalyst (1 mol%), 340 g 4-phenylmorpholine

(2.09 mol) and deuterium oxide (1,500 ml, 83 mol) were added. The autoclave was flushed with hydrogen six times at 10 bar and finally pressurized to the desired value (20 bar). Then, it was placed into an equipment (see Supplementary Section 9 for more details) for the autoclave and heated to 120 °C, and then held at 120 °C for 120 h. At the end of the reaction, the autoclave was quickly cooled down to r.t. with an ice bath and vented. Finally, the crude reaction was added to ethyl acetate (1.5 l). The reaction mixture was filtered with filter paper. The D_2O layer was removed from the mixture and washed with ethyl acetate (1.5 l, three times). After removal of all volatiles in vacuo, 341 g of deuterium product was obtained. It is important to note that during the cool down, trace amounts of gas can stay in the solid phase (product and catalyst). Thus, the solid phase should be dissolved slowly in ethyl acetate.

Data availability

All data generated or analysed in this study are available in this article and its Supplementary Information.

Acknowledgements

We thank the analytical staff of the Leibniz-Institute for Catalysis, Rostock, for their excellent service, specifically W. Baumann for his accurate quantitative ^1H NMR analysis, R Jackstell for offering the 2 l autoclave and D.K. Leonard for assistance in the preparation of the manuscript. We gratefully acknowledge support from the Federal Ministry of Education and Research (BMBF), the State of Mecklenburg-Vorpommern, EU (FLIX project) and the European Research Council (ERC; project NoNaCat 670986).

Author contributions

M.B. and W.L. conceived and designed the project. W.L. and F.B. developed and prepared the catalysts and performed all catalytic experiments and analysed the data. A.B. and J.R. were responsible for the EPR experiments. D.Y. and A.L. were responsible for the XAFS experiments. C.K. and N.R. were responsible for the TEM experiments. H.L. was responsible for the X-ray diffraction experiments. S.B. was responsible for the XPS experiments. K.J., A.-E.S. and A.B. participated in the discussions and supported the project. W.L., J.R., A.B. and M.B. co-wrote the paper.

Competing interests

The authors declare no competing interests.

Additional information

Supplementary information The online version contains supplementary material available at <https://doi.org/10.1038/s41557-021-00846-4>.

Correspondence and requests for materials should be addressed to Angelika Brückner, Aiwen Lei or Matthias Beller.

Peer review information *Nature Chemistry* thanks Marc Reid and the other, anonymous, reviewer(s) for their contribution to the peer review of this work.

Reprints and permissions information is available at www.nature.com/reprints.